

# Thermal Enhancement of Parabolic Trough Collectors using Absorber Tubes with Internally longitudinal Round Edge Fins

Nourhan B. Saad<sup>a</sup>, Antar M M Abdala<sup>a</sup>, M. Fatouh<sup>a, b</sup>

a. Mech. Power Eng. Dep., Fac. of Eng. @ El-Mattaria, Helwan Uni., Masaken El-Helmia  
P.O., Cairo 11718, Egypt.

b. High Institute for Eng. & Tech. - Obour, k21 Cairo/Belbies Rd, Egypt

## Abstract

In this paper, the heat transfer characteristics of the absorber tube with the module of LS-2 parabolic trough collector with internal longitudinal fins with rectangular cross-section are investigated using ANSYS CFD and oil syltherm 800 type as a heat transfer fluid. The simulation is conducted using the internal longitudinal fins with sharp edge and round edge over a wide range of the heat transfer fluid inlet temperature (300 :600K), flow rate (9 :27 m<sup>3</sup>/h) and direct normal irradiance (800:1100W/m<sup>2</sup>) at fin thickness of 4 mm, fin length of 25 mm, radius of round edge of 4 mm and angle between fins of 45°. The thermal efficiency, Nusselt Number, pressure losses, and thermal enhancement index are calculated at different operating conditions. The results showed that the heat transfer characteristics of rectangular fins with round edge are better than those with sharp edge in solar parabolic trough collector. The round edge fins yield higher Nusselt number and lower pressure losses than those of the sharp edge fins by 5.6% and 9.32%; respectively, at inlet temperature of 600 K, oil flow rate of 9 m<sup>3</sup>/h., and direct normal irradiance of 1000W/m<sup>2</sup>.

**Keywords:** Rectangular finned absorber; round edge; non- uniform heat flux; thermal enhancement index; pressure losses; thermal efficiency.

## 1. Introduction

The parabolic trough collector (PTC) is a type of solar thermal concentrator that is used to generate heat at high and medium temperatures. PTC uses troughs or curved mirrors to focus solar energy onto receiver tubes placed at the trough's focal length. The receiver is made up of an absorber tube contained within an evacuated glass chamber. The absorber tube, which is typically made of stainless steel, has a spectrally selective surface coating that maximizes solar irradiation absorption while reducing heat loss by emitting less radiation. A heat transfer fluid (HTF) is circulated in the focal length tubes and then pumped through a series of heat exchangers to produce heat with temperature ranges from 200 to 400°C for use in various applications. PTC's performance is influenced by its geometric parameters, which

include the absorber tube/receiver and glass cover (GC) diameters, as well as the rim angle, aperture width, focal length, and concentration ratio. Among these geometric parameters, the absorber tube has an important role in heat transfer enhancement of PTC. Heat transfer enhancement methods for the absorber tube of PTC can be classified into active and passive methods [1]. There is no external force used in the passive approach to improve heat transfer. Typical inserts such as twisted tapes, wire coils, metal foams, and discs are used to improve heat transfer caused by a reduction in the thickness of the thermal boundary layer, as well as an increase in turbulence and a velocity gradient near the walls. However, internal longitudinal fins inside the absorber tube were utilized to increase the rate of heat transfer.

Jaramillo et al., [2] investigated the effect of employing twisted tape for heat transfer augmentation in a PTC through series of experiments and numerical simulations. They showed that when the twist ratio was near to 1 and the Reynolds number was low, using twisted tape increased heat transfer. The use of wall detached twisted tape inserts in a PTC was reported by Mwesigye et al., [3]. The results showed that the heat transfer performance increased by 169% and the thermal efficiency increased up to 10% over a receiver with smooth tube in their study. Chang et al. [4] studied the influence of twist ratios (2.5:41.7) and clearance ratios (0:1) for twisted tape on PTC performance in turbulent flow with Re (7485-30553). Ghadirijafar et al., [5] provided a numerical analysis of different tape inserts with distinct twist ratios of 2.67, 4, and 5.33, in a PTC's absorber tube. They confirmed that the whirling flow of the twisted tape combined with the vortex formed by the louvered fins results in a significant increase in heat transfer. Garg et al. [6] reviewed previous work in the field of heat transfer augmentation using twisted tapes. They discovered that in turbulent flow, twisted tapes do not perform well over a wide range of Reynolds numbers, resulting in a large pressure drop due to flow blockage.

Diwan and Soni [7] investigated the effect of wire coil inserts in a PTC absorber tube, with flow rates ranging from 0.01388 kg/s to 0.099 kg/s at a constant water inlet temperature of 313 K for pitch values of 6 mm, 7 mm, 8 mm, 9 mm, 10 mm, 12 mm, 15 mm, 17 mm, and 20 mm. Due to heat transfer enhancement and friction factors in the absorber tube, pitch values of 6–8 mm were preferred for lower flow rates, whereas pitch values of 8mm were suitable for higher flow rates. Sahin et al. [8] investigated the use of a wire coil insert within a water-filled absorber tube. They discovered that, for pitch distance (15, 30 and 45mm), the heat transfer enhancements were 2.28, 2.07 and 1.95 times; respectively higher than the smooth tube.

The effect of metal foam on the thermal efficiency of a PTC absorber tube was investigated by Jamal-Abad et al. [9]. The tests were carried out in accordance with the ASHRAE 93 standard, with flow rates ranging from 0.5 to 1.5 Lit/min and copper foam with a porosity of 0.9 and a density of 30 PPI being used (pores per inch). They reported that the overall loss coefficient decreased by 45% when the absorber filled with the metal foam and the thermal efficiency increased due to less energy lost. Rashidi et al. [10] examined the use of porous materials in solar energy systems. They discovered that porous materials have a positive impact on heat transfer but a negative

impact on pressure drop and, as a result, pumping power. Ghasemi and Ranjbar [11] investigated the use of porous rings inside a Syltherm 800 absorber and discovered that the heat transfer characteristic increased when the distance between porous rings decreased. Chang et al. [12] investigate the use of an eccentric rod insert in an absorber. They discovered that, when dimensionless diameter increased from 0.1 to 0.09, the performance evaluation criteria is about 1.12 to 3.38 times than for the plain parabolic trough receiver at Re of  $1 \times 10^4$ . The use of a star flow insert in a PTC was suggested by Bellos and Tzivanidis [13]. They stated that the thermal efficiency can be improved by 1%. Mwesigye et al. [14] investigated the effect of the perforated plate insert on PTC performance numerically. They found that the entropy generation rates are reduced by 53% with heat transfer enhancement, when the Re below the optimal value. Bellos et al., [15] evaluated the usage of internally finned absorbers with sharp edges in the LS-2 PTC. Twelve different fin cases were tested. They concluded that when compared to the smooth case, the thermal efficiency is enhanced by 0.82 %, the Nusselt number is increased by 65.8%, and the friction factor and pressure losses are doubled for the optimum case of the absorber with fin length 10mm and fin thickness 2mm. Cheng et al., [16] investigated the use of longitudinal vortex generators in the absorber's down section. Their results revealed that for each geometric parameter, the average Nusselt number and the average friction increased, while the average wall temperature and the thermal loss decreased. Moreover, the number and location of internal longitudinal fins inside the absorber tube were optimized by Bellos et al., [17] with Syltherm 800 as a working fluid at a constant flow rate of 150 L/min. They indicated that the best design contains three fins in the down section, which results in a 0.51 % increase in thermal efficiency. Munoz and Abanades [18] investigated the usage of helical fins inside the absorber and discovered that using Syltherm 800 as a working fluid increased thermal efficiency by 3%. Bellos et al., [19] studied the use of converging-diverging absorber tube shape for working with thermal oil. This improvement causes the thermal efficiency to increase by 4.55 %. Bellos et al., [20] investigated the use of internally finned absorbers in the LS-2 PTC. Twelve distinct fin cases were evaluated under a wide range of the inlet temperature (300: 600 K). The base fluid was thermal oil with flow rate of 150L/min. For inlet temperature of 600 K, the increase in thermal efficiency and the thermal enhancement index were 1.27 % and 1.483; respectively. Laaraba et al. [21] studied an internally finned absorber, the LS-2 PTC, with fins in the lower half of the absorber tube and a total of 5 fins of varying thickness and length. They showed that by modifying the surface in this way, the thermal enhancement index could be increased to 1.6 for fin length 15mm and fin thickness 6mm.

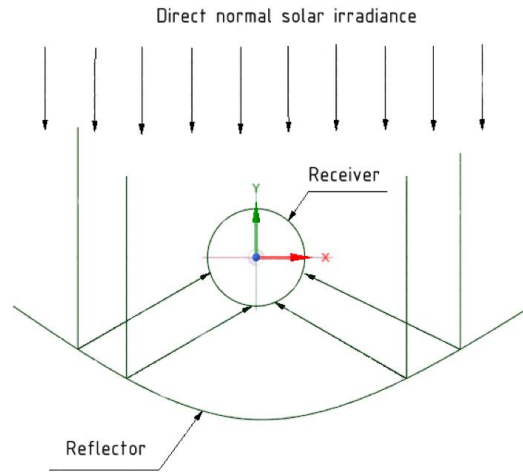
The above literature review reveals that twisted tapes, wire coils, metal foams, and discs are used to improve heat transfer. Also, the internal fins are considered as one of the most efficient techniques to enhance heat transfer of the absorber tube. The internal rectangular fins with sharp edge are tested over a narrow range of flow rate at constant direct normal solar irradiance ( $1000\text{W}/\text{m}^2$ ) [22]. However, there is a lack of studies which compare internal fins with sharp edge and round edge over a wide range of operating conditions. In the current work, the use of internal rectangular fins

with round and sharp edge inside the absorber is investigated using ANSYS CFD over a wide range of inlet temperature (300:600 K), heat transfer fluid flow rate (9:27 m<sup>3</sup>/h) and direct normal solar irradiance (800:1100 W/m<sup>2</sup>) using fin length of 25mm, fin thickness of 4mm, radius of round edge of 4mm and the angle between fins of 45°.

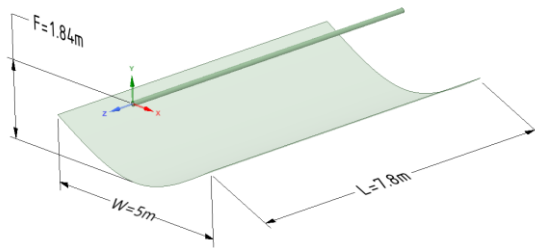
## 2. Physical model

Figure (1) indicates the main parts of LS-2 parabolic trough concentrator, which is used in the current work. The thermal concentrator of standard parabolic trough consists of a reflector (linear parabolic mirror) and an evacuated tube (receiver). The reflector has a reflectivity of 0.83 while the evacuated tube includes stainless steel absorber and glass cover. The absorber tube has inner diameter of 66 mm, outer diameter of 70 mm, and surface absorptivity ( $\alpha$ ) of 0.96. The glass cover has inner diameter of 109 mm, outer diameter of 115 mm, transmissivity ( $\tau$ ) of 0.95, and emissivity ( $\varepsilon$ ) of 0.86 [20]. PTCs use direct solar radiation, called direct normal irradiance (DNI), which comes directly from the sun. The linear parabolic mirror reflects and concentrates the received solar energy onto the receiver positioned along the focal line of PTC as shown in Fig 1. The incident rays are collected by the receiver tube, which converts them into heat that is carried by heat transfer fluid through the absorber tube. As shown in Fig 2, the LS-2 parabolic trough module has a focal length of 1.84 m, a parabola width and length of 5 m and 7.8 m; respectively, a total aperture area ( $A_a$ ) of 39 m<sup>2</sup> and concentration ratio ( $C=A_a(39)/A_{ro}(1.715)$ ) of 22.74. Because of various optical losses as tracking error and possible manufacturing error, the final optical losses value is 0.755 as reported by Behar et al. [23]. The details of LS-2 parabolic trough are available in literature [24]. The model is simplified by assuming the incident angle is zero, vacuum pressure in the glass envelope, and radiation exchange between the absorber surface and the glass envelope is almost negligible.

The current work aims to enhance the heat transfer characteristic of the absorber tube for PTC using turbulators, which have internally rectangular longitudinal fins with round edge and shape edge at fin thickness ( $t$ ) of 4 mm, length ( $p$ ) of 25 mm, radius ( $R$ ) of the round edge of 4 mm and angle between fins ( $\theta$ ) of 45° as shown in Fig 3. Wide ranges of inlet temperatures (300: 600 K), heat transfer fluid flow rates (9: 27 m<sup>3</sup>/h) and a direct normal irradiance (800:1100W/m<sup>2</sup>) are used in the present work.



**Figure 1 Schematic diagram of a solar parabolic trough concentrator**



**Figure 2 Standard LS-2 parabolic trough concentrator**

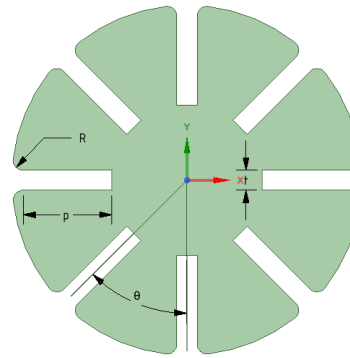


**Figure 3 Internally rectangular longitudinal fins with round edge shape (present model)**

### 3. Computational fluid dynamics model

The governing equations of mass conservation, momentum conservation, and energy conservation are solved in each cell by CFD code (FLUENT version 18.2) and two user-defined functions (UDFs) are used to calculate the heat flux wall boundary condition for the tube wall using the input solar flux. For turbulent flow, these governing equations are modeled by Reynolds Averaged Navier-Stokes (RANS) equations, which based on a finite control volume approach that employs a structured mesh to achieve high node resolution.

The present fluid domain is validated using three different turbulence models namely,  $k-\epsilon$ ,  $k-\omega$  and SST with Dudley et al. [24] as shown in Fig 4. The average deviation in the thermal efficiency for the turbulence  $k-\epsilon$ ,  $k-\omega$  and SST models are 2.74%, 2.7371% and 2.7360%; respectively, while their computation times are 8 h, 11 h and 12 h; respectively. Therefore, the appropriate turbulence model for the present fluid domain is Realizable  $k-\epsilon$  model due to its low computation time.

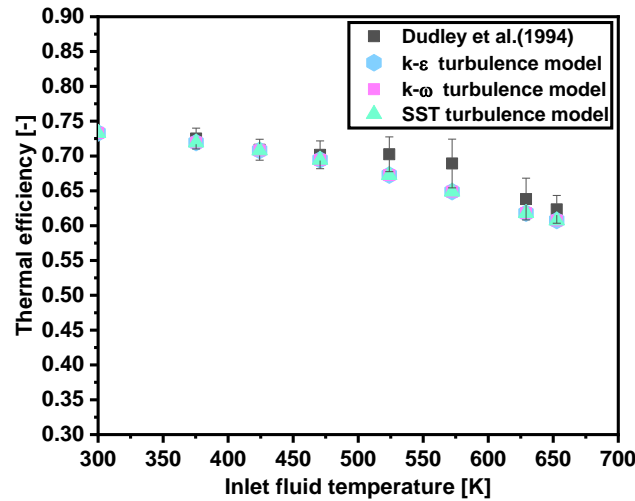


Figure 4 Comparison between three turbulence models and experimental results to select the best turbulence model

#### 4. Mathematical model and Boundary conditions of CFD analyses

##### 4.1 Boundary conditions of CFD analyses

The inlet boundary conditions are the flow rate and the inlet temperature of thermal oil as listed in Table 1. The outlet is fully developed flow. Thermal oil is used as a heat transfer fluid in present work and its properties are reported in literature [20].

Table 1. Boundary condition of the present work

Boundary Condition	Values
Inlet	The inlet temperature, $T_{in}$ (300-600) K The volume flow rate, $V$ (9-27) $m^3/h$
Outlet	Fully developed flow and zero pressure gauge
Outer wall	Non-uniform heat flux with DNI (800-1100) $W/m^2$

##### 4.2 Mathematical model

The available solar irradiation on the collector aperture  $Q_s$  [W] is defined by Eq. (1).

$$Q_s = A_a \cdot I_b \tag{1}$$

Where  $A_a$  is the total aperture area of  $39 m^2$  and  $I_b$  is the direct normal irradiance. The useful heat ( $Q_u$ ) captured by the fluid is calculated according to the energy balance in the fluid volume and is defined by Eq. (2).

$$Q_u = \dot{m} \cdot c_p \cdot (T_{out} - T_{in}) \tag{2}$$

Where,  $\dot{m}$  is the flow rate of working fluid,  $c_p$  is the specific heat of working fluid,  $T_{in}$  is the inlet temperature of working fluid, and  $T_{out}$  is the outlet temperature of the working fluid and it's known by the computational tool.

The PTC thermal efficiency ( $\eta_{th}$ ) of the solar collector is defined as the ratio of the useful heat ( $Q_u$ ) to the available solar irradiation ( $Q_s$ ).

$$\eta_{th} = \frac{Q_u}{Q_s} \quad (3)$$

The PTC thermal losses ( $Q_{loss}$ ) from the absorber tube can be calculated from the following equation

$$\frac{Q_{loss}}{Q_s} = \eta_{opt} - \eta_{th} \quad (4)$$

It may be stated that the optical efficiency ( $\eta_{opt}$ ) value is 0.755 as reported by Behar et al. [21]. The heat transfer coefficient ( $h$ ) between the absorber tube and the working fluid can be calculated by Eq. (5). In this equation, the useful heat  $Q_u$  is calculated from Eq (2), the receiver mean temperature  $T_r$  [K] is known by the computational tool, as well as the mean fluid temperature  $T_{fm}$  [K] is calculated from Eq. (6).

$$h = \frac{Qu}{(\pi \cdot D_{ri} \cdot l) \cdot (T_r - T_{fm})} \quad (5)$$

Where  $l$  and  $D_{ri}$  are the length and diameter of the absorber and the mean fluid temperature can be estimated as:

$$T_{fm} = \frac{(T_{in} + T_{out})}{2} \quad (6)$$

The Nusselt number ( $Nu$ ) is calculated using the heat transfer coefficient using the following equation.

$$Nu = \frac{h \cdot D_{ri}}{K} \quad (7)$$

Where  $K$  is the thermal conductivity of working fluid. The friction factor ( $f$ ) is calculated using Eq. (8), which is reported by Bellos et al. [20] as a function of the pressure losses ( $\Delta p$ ) along the absorber tube are known by the computational tool and  $\rho$  is the density of working fluid,  $u$  is the mean velocity of working fluid.

$$f = \frac{\Delta p \cdot 1000}{\frac{1}{2} \cdot \rho \cdot u^2} \cdot \left(\frac{D_{ri}}{l}\right) \quad (8)$$

The thermal enhancement index ( $TEI$ ) is defined according to Eq (9). This index is the main factor to compare the different configurations of finned absorber with smooth absorber which takes into consideration the Nusselt enhancement in addition to the friction factor increase, which corresponds to the same pumping power consumption. When this index is over 1, then the examined case is better thermal performance compared to the respective reference case.

$$TEI = \frac{Nu / Nu_0}{\left(\frac{f}{f_0}\right)^{1/3}} \quad (9)$$

Where  $Nu$  refers to Nusselt number of the finned absorber,  $Nu_0$  refers to Nusselt number of the respective reference case which means the smooth absorber,  $f$  refers to friction factor of the finned absorber and  $f_0$  refers to friction factor of the respective reference case.

## 5. Meshing and model validation

### 5.1 Mesh independent study

Figure 5 indicates 3D view of structured hexahedral mesh for used meshing of absorber tube in the current research. The grid independence verification test is performed on six different grid cells: 300,000, 600,000, 800,000, 1,076,400, 2,630,880, and 3,700,000. Table 2 compares the grid independence verification tests for the heat transfer fluid's outlet temperature to the experimental results [24]. Clearly, the mesh size of 2,630,880 produces accurate results as given in Table 2. Hence it was used throughout the validation and present work.

### 5.2 Model validation

The simulated model is validated against experimental data reported by Dudley et al. [24] for the smooth absorber tube. Figure 6 shows a comparison between experimental thermal efficiency data of Dudley et al. [24] and thermal efficiency data of the present model for the smooth absorber tube. It is found that the average deviation is relatively low, about 2.74 %.

**Table 2 Grid independence tests**

Parameters	Mesh1	Mesh2	Mesh3	Mesh4	Mesh5	Mesh6
No of cells	300,000	600,000	800,000	1,076,400	2,630,880	3,700,000
$T_{out}$ (Present work)	559.5	552.4	547.2	545.987	545.575	545.569
$T_{out}$ (EXP)	542.6	542.6	542.6	542.6	542.6	542.6
error %	-3.115	-1.806	-0.848	-0.624	-0.548	-0.547

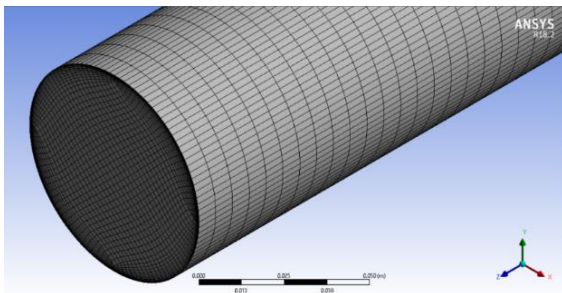


**Figure 5 3D view of structured hexahedral mesh for used meshing of absorber tube**

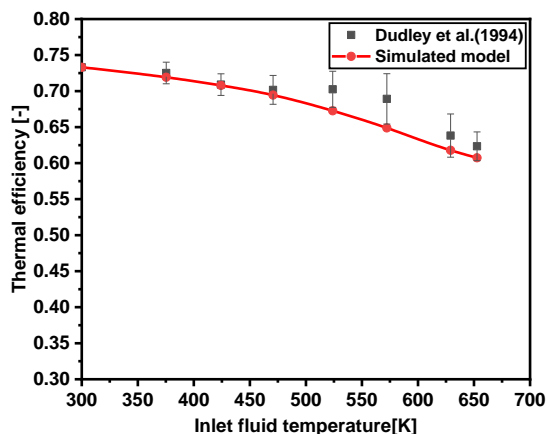


**Figure 6 Comparisons between the present model and experimental results for validation**

## 6. Results and discussion

### 6.1. Smooth tube results

In order to make a comparison between different configurations of finned absorber tubes based on the thermal enhancement index ( $TEI$ ), smooth absorber tube data must be available. Consequently, useful heat, thermal efficiency, thermal losses of the PTC and pressure losses along the tube for smooth absorber tube are given in Table 3 while heat transfer coefficient, Nusselt number and friction factor for smooth absorber tube are presented in Figs. (10-12).

**Table 3 Performance characteristics of smooth absorber tube**

Inlet temp [K]	Useful heat [kW]	Thermal efficiency [-]	Thermal loss [kW]	Pressure loss [kPa]
300	29.289	0.751	0.156	1.057
350	29.172	0.748	0.273	0.807
400	28.977	0.743	0.468	0.676
450	28.665	0.735	0.780	0.562
500	28.236	0.724	1.209	0.466
550	27.534	0.706	1.911	0.412
600	26.598	0.682	2.847	0.341

### 6.2 Effect of edge type

The effect of the edge type of internal longitudinal fins with rectangular shape inside the absorber tube is investigated over a wide range of inlet fluid temperature ranges from 300 K to 600 K with step 50 K, while the fin length, thickness, and radius of round edge remain unchanged at 25mm, 4mm and 4mm; respectively, in addition to the angle between fins, flow rate and direct normal irradiance are kept constant at 45°, 9m<sup>3</sup>/h, 1000 W/m<sup>2</sup>; respectively.

Useful heat, the thermal efficiency, the thermal losses of the PTC and the pressure losses along the absorber tube as a function of inlet fluid temperature are given in Table 4 for the round and sharp edges. The higher useful heat is created when round edge fins is used because it creates higher turbulence in the fluid flow and improves the performance of the absorber. Fin of round edge yields higher thermal efficiency than that of sharp edge as listed in Table 4. This is because of fin of round edge has higher useful heat at the same direct solar irradiance. Table 4 reveals that the lower thermal loss is achieved using fin with round edge. This is because of round edge fins create higher heat transfer than that in the sharp edge. The pressure loss along the absorber when used round edge is lower than that in the sharp edge as tubulated in Table 4. It may be concluded that thermal loss of the round edge is lower than that of the sharp edge by about 33.3% at inlet fluid temperature of 400K and the pressure losses are 2.50 kPa and 2.665 kPa for the round and sharp edge; respectively at 500K inlet fluid temperature.

Figure 10A illustrates the heat transfer coefficient for both finned (with round edge and sharp edge) and smooth absorber tubes against inlet fluid temperature. It indicates

that the highest heat transfer coefficient is achieved when round edge is used. This is because of round edge creates higher turbulence in the flow and good mixing than that occur in the sharp edge. At the inlet fluid temperature of 450K, the fins with round edge yield heat transfer coefficient of 1600 W/m<sup>2</sup>K, while the fins with sharp edge achieve heat transfer coefficient of 1388 W/m<sup>2</sup>K. The Nusselt number as a function of the inlet fluid temperature for round edge and sharp edge as well as smooth tube is shown in Fig. 10B. Clearly, the higher Nusselt number is achieved using round edge fins due to its higher heat transfer coefficient than that in the sharp edge. The round edge fins have higher Nusselt number than that of the sharp edge fins by nearly 6.35% at the inlet fluid temperature of 450K.

Figure 10C depicts the friction factor for smooth tube and finned tube with round edge and sharp edge. It is observed that the friction factor is getting lower for round edge fins than that for the sharp edge. The sharp edge yields higher friction factor than that of the round edge by 25.2% at the inlet fluid temperature of 500 K. Change of the thermal enhancement index against inlet fluid temperature is illustrated in Fig. 10D, which indicates that the round edge has better performance than that of the sharp edge over the whole range of inlet fluid temperature. This can be attributed due to higher Nu number (see, Fig. 10B) and lower friction factor (see, Fig. 10C) of the round edge than that of sharp edge for given inlet fluid temperature. Thermal enhancement index of the round edge is higher than that of the sharp edge by about 13.8% at inlet fluid temperature of 600K.

### 6.3 Effect of inlet fluid temperature

The effect of inlet fluid temperature ( $T_{in}$ ) is investigated at the fin length of 25mm, fin thickness of 4mm and round edge radius of 4 mm, angle between fins of 45°, flow rate of 9 m<sup>3</sup>/h and direct normal irradiance of 1000 W/m<sup>2</sup>.

Table 4 tabulate the useful heat, the thermal efficiency, the thermal losses and the pressure losses along the absorber for the finned absorber tube with round and sharp edge as a function of the inlet fluid temperature. Clearly, useful heat, thermal efficiency and pressure loss are inversely proportional while thermal loss is directly proportional to inlet fluid temperature. This is because of higher inlet fluid temperature leads to lower heat absorbed by the working fluid then the useful heat and thermal efficiency are low. As the inlet fluid temperature increases from 300 to 600K, the useful heat decreases from 29.406 kW to 27.006 kW; respectively, for round edge and from 29.367 kW to 26.949 kW; respectively, for sharp edge. The thermal efficiency is reduced by nearly 8.64 and 8.97% for round and sharp edge; respectively, as the inlet fluid temperature increases from 300 to 600K. Inspection in Table 4 reveals that higher inlet fluid temperature leads higher thermal losses due to lower thermal efficiency and vice versa. For the sharp edge fins, inlet fluid temperature of 300K and 600K yields the lower (0.078 kW) and higher (2.496 kW) value of thermal losses; respectively. The pressure losses decrease with inlet fluid temperature increase as listed in Table 4. This is because of the higher inlet fluid temperature levels lead lower dynamic viscosity. The pressure losses are 5.489 and

2.2 kPa at the inlet fluid temperature of 300 and 600 K; respectively, for the sharp edge fins.

Figure 10A illustrates the heat transfer coefficient against the inlet fluid temperature. It is seen that higher inlet fluid temperature leads higher convection heat transfer coefficient. When the inlet fluid temperature increases from 300 and 600K, the heat transfer coefficient value increases from 550 to 1950 W/m<sup>2</sup>K; respectively, for the round edge fins, and from 250.26 to 664.72 W/m<sup>2</sup>K; respectively, for the smooth absorber. The Nusselt number as a function of inlet fluid temperature for smooth absorber tube and finned absorber tube with round edge and sharp edge is shown in Fig 10B, which proves that Nusselt number increases with higher inlet fluid temperature. As inlet fluid temperature changes from 300 to 600 K, the Nusselt number increases from 277 to 1643; respectively, for the round edge fins and from 123.539 to 567.55; respectively, for the smooth absorber tube. Fig 10C indicates the friction factor against the inlet fluid temperature for the smooth tube and finned tube with round edge and sharp edge. The friction factor is low at high inlet fluid temperatures due to low dynamic viscosity. Clearly, inlet fluid temperature of 300K yields higher friction factor compared the inlet fluid temperature of 600K for smooth. The friction factor is nearly 0.152 and 0.088 at the inlet fluid temperature of 300 and 600 K; respectively, for the round edge fins. The smooth absorber has friction factor of 0.037 and 0.016 at inlet fluid temperature of 300 and 600 K; respectively. Fig 10D shows variation of the thermal enhancement index with the inlet fluid temperature. It is seen that the thermal enhancement index increases with the inlet fluid temperature increase. This is mainly due to the trend of both Nusselt number and friction factor as earlier discussed. The thermal enhancement index is approximately 1.64 and 1.4 at the inlet fluid temperature of 600 and 300 K for the round edge fins.

**Table 4 Performance characteristics of finned tube as a function of inlet temperature**

Inlet temp [K]	Useful heat [kW]		Thermal efficiency [-]		Thermal loss [kW]		Pressure loss [kPa]	
	round	sharp	round	sharp	round	sharp	round	sharp
T <sub>in</sub>								
300	29.406	29.367	0.754	0.753	0.039	0.078	5.280	5.489
350	29.367	29.289	0.753	0.751	0.078	0.156	3.600	3.781
400	29.211	29.094	0.749	0.746	0.234	0.351	3.200	3.386
450	28.977	28.860	0.743	0.740	0.468	0.585	2.850	3.102
500	28.548	28.431	0.732	0.729	0.897	1.014	2.500	2.665
550	27.924	27.807	0.716	0.713	1.521	1.638	2.160	2.312
600	27.066	26.949	0.694	0.691	2.379	2.496	1.995	2.200

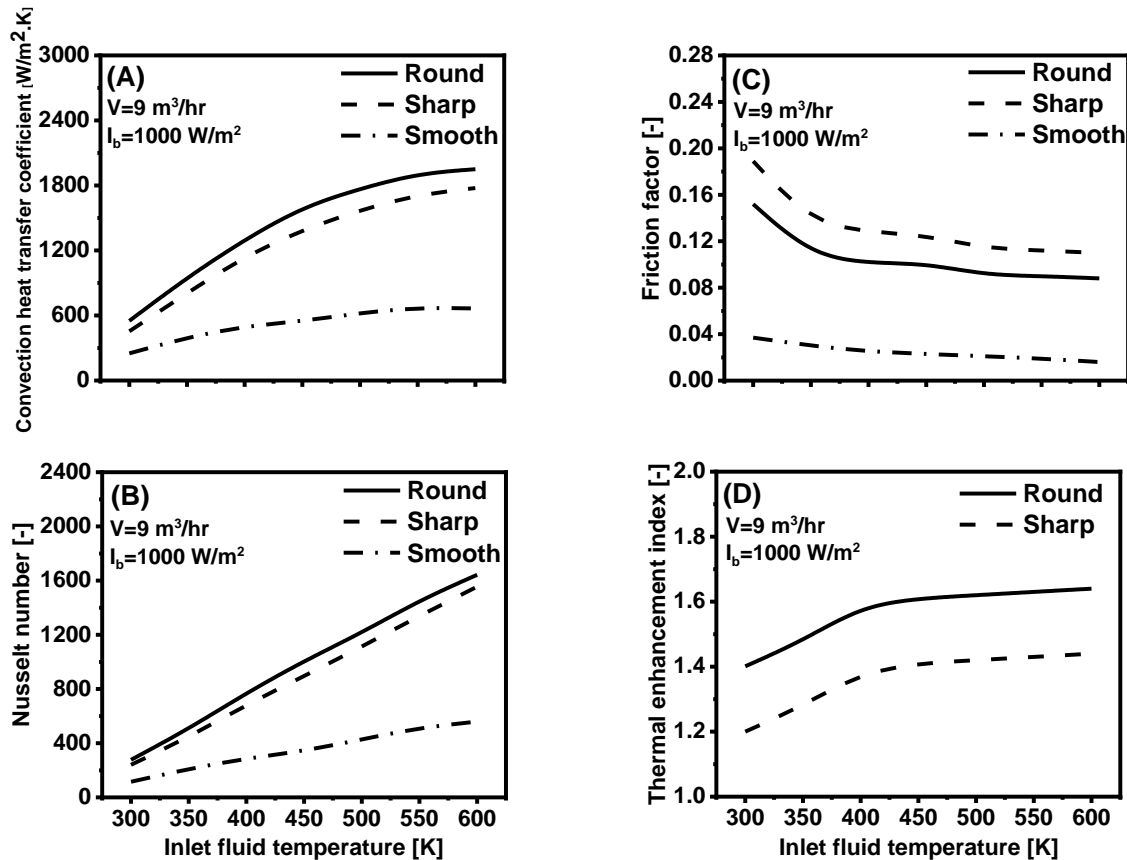


Figure 10 Variation of performance characteristics with inlet fluid temperature for different edges

### 6.4 Effect of volume flow rate

The effect of volume flow rate ( $V$ ) is investigated when the fin length, thickness and radius of round, angle between fins, the inlet fluid temperature and direct normal irradiance are kept constant.

Table 5 lists the useful heat, thermal efficiency, the thermal losses and the pressure losses along the absorber tube for the round and sharp edge as a function of volume flow rate. Higher flow rate leads to higher useful heat. Table 5 reveals that as volume flow rate increases, the useful heat, thermal efficiency, and the pressure losses increase while the thermal losses decrease. Thermal efficiency increases when flow rate increases because it has higher useful heat at the same direct solar irradiance. The higher flow rate leads lower thermal losses due to larger heat absorption capability. The pressure losses increase along the absorber when higher volume flow rate level is used because the higher volume flow rate levels cause higher turbulence. As volume flow rate varies from 9 to 27  $\text{m}^3/\text{h}$ , the useful heat changes from 27.066 kW to 28.002 kW and from 26.949 kW to 27.882 kW for round edge and for the sharp edge; respectively. The thermal efficiency of the round edge is 0.694 and 0.718, while for sharp edge case is 0.691 and 0.715 at the volume flow rate of 9 and 27  $\text{m}^3/\text{h}$ ; respectively. Thermal losses at the volume flow rate of 27  $\text{m}^3/\text{h}$  are lower than that at the volume flow rate of 9  $\text{m}^3/\text{h}$  by about 39.3% and 37.379% for the round edge and

sharp edge; respectively. The pressure losses increase from 1.995 kPa to 12.86 kPa for the round edge and from 2.2 kPa to 14.182 kPa for the sharp edge when the volume flow rate increases from 9m<sup>3</sup>/h to 27m<sup>3</sup>/h.

The heat transfer coefficient against volume flow rate for the smooth tube and finned tube with sharp edge and round edge is presented in Fig. 11A. The round edge fins achieve heat transfer coefficient (HTC) from 1950 W/m<sup>2</sup>K to 3535 W/m<sup>2</sup>K and the sharp edge fins yield HTC from 1775.8 W/m<sup>2</sup>K to 3219 W/m<sup>2</sup>K as the volume flow changes from 9m<sup>3</sup>/h to 27m<sup>3</sup>/h.

Figure 11B indicates the Nusselt number as a function of volume flow rate for smooth and finned tubes. Nusselt number is directly proportional to the volume flow rate. This is mainly due to the trend of heat transfer coefficient with the volume flow rate. Nusselt number increases from 1643 to 3000 for the round edge fins and from 1555.72 to 2839.8 for the sharp edge when the volume flow rate increases from 9m<sup>3</sup>/h to 27m<sup>3</sup>/h.

Figure 11C presents the friction factor versus the volume flow rate for the sharp edge and round edge as well as the smooth tube. It is observed that the friction factor is inversely proportional to the volume flow rate. The friction factor values from 0.07 to 0.088 for the round edge and from 0.087 to 0.11 for the sharp edge for volume flow rate from 9m<sup>3</sup>/h to 27m<sup>3</sup>/h. The variation of thermal enhancement index with different values of volume flow rate for the sharp edge and round edge is illustrated in Fig. 11D, which indicates that the best thermal enhancement index is 1.64 and 1.44 for the round and sharp edge, respectively, at 9 m<sup>3</sup>/h.

**Table 5 Performance characteristics of finned tube as function of a mass flow rate**

Flow rate [m <sup>3</sup> /h]	Useful heat [kW]		Thermal efficiency [-]		Thermal loss [kW]		Pressure losses [kPa]	
	round	sharp	round	sharp	round	sharp	round	sharp
V								
9	27.066	26.949	0.694	0.691	2.379	2.496	1.995	2.200
12	27.417	27.299	0.703	0.700	2.028	2.145	3.205	3.534
15	27.768	27.649	0.712	0.709	1.677	1.796	4.370	4.819
18	27.846	27.726	0.714	0.711	1.599	1.718	6.078	6.703
21	27.924	27.804	0.716	0.713	1.521	1.641	8.095	8.927
24	27.963	27.843	0.717	0.714	1.482	1.602	10.206	11.255
27	28.002	27.882	0.718	0.715	1.443	1.563	12.860	14.182

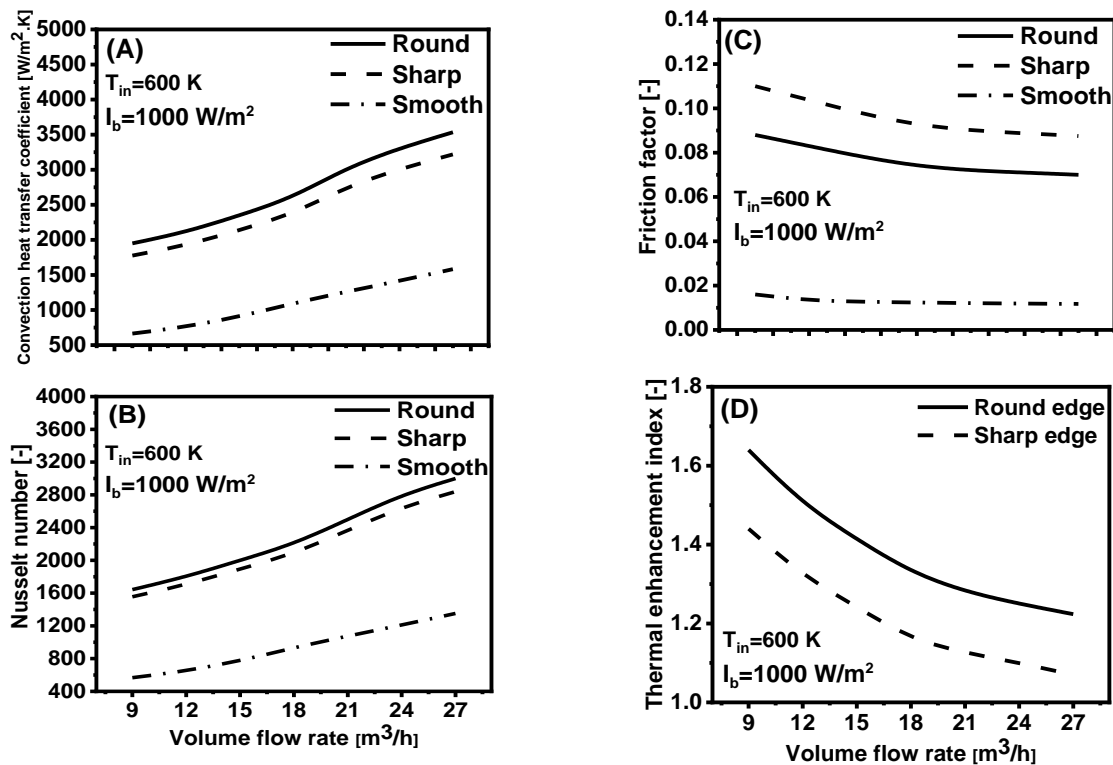


Figure 11 Variation of performance characteristics with volume flow rate for different edge

## 6.5 Effect of incident solar radiation

The influence of incident solar irradiation ( $I_b$ ) on thermal performance of PTC in a typical working condition is reported and discussed when the volume flow rate and inlet temperature of thermal oil are 9 m<sup>3</sup>/h and 600 K; respectively, the fin length, thickness and radius of round edge are 25mm, 4mm and 4mm respectively, and angle between fins is 45°.

The useful heat, thermal efficiency, thermal losses and pressure losses along the absorber tube versus incident solar radiation for the round and sharp edge are given in Table 6. Higher incident solar radiation leads to higher useful heat as it expected. As solar radiation intensity ( $I_b$ ) rises from 800 to 1100 W/m<sup>2</sup>, the useful heat varies from 21.4254 kW to 29.743 kW for the round edge fins and from 21.333 kW to 29.616 kW for the sharp edge fins. The thermal efficiency and the thermal loss ( $Q_{loss}$ ) increase as  $I_b$  increase if other operating conditions are kept constant. This can be explained as follows; when the  $I_b$  increases for given operating parameters, the absorber couldn't absorb all the direct normal irradiance that arriving at the absorber, so the wall temperature of the absorber increases and corresponding  $Q_{loss}$  increases. The round edge fin has thermal efficiency increases from 0.6867 to 0.69332 and thermal losses increases from 2.13 kW to 2.646 kW while the sharp edge has thermal efficiency increases from 0.6837 to 0.6903 and thermal losses increases from 2.223 kW to 2.773 kW as solar radiation intensity changes from 800 W/m<sup>2</sup> to 1100 W/m<sup>2</sup>. The pressure losses decrease along the absorber tube when used higher incident solar radiation because higher incident solar radiation leads lower dynamics viscosity. The

pressure losses at the solar radiation intensity of  $800\text{W/m}^2$  is higher than that at the solar radiation intensity of  $1100\text{W/m}^2$  by about 76.47% and 76.42% for the round and sharp edge fins; respectively.

The heat transfer coefficient as a function of incident solar radiation for the smooth tube in addition to the sharp and round edge finned tube is illustrated in Fig. 12A. It is seen that higher solar radiation leads higher heat transfer coefficient due to larger heat absorption capability. Heat transfer coefficient at solar radiation of  $1100\text{W/m}^2$  is higher than that at solar radiation of  $800\text{W/m}^2$  by 33.39% and 33.42% for the round edge and sharp edge fins; respectively. Figure 12B presents the Nusselt number against incident solar radiation for different type of tubes. This figure shows that the higher Nusselt number increases with using the round edge fin. This is because the round edge fins have higher heat transfer coefficient so the Nusselt number increase with solar radiation increase, as shown in Fig 12B. Nusselt number varies from 1378.2 to 1838.6 for the round edge fins and from 1304.41 to 1739.85 for the sharp edge fins as incident solar radiation increases from  $800\text{ W/m}^2$  to  $1100\text{ W/m}^2$ .

Figure 12C indicates the friction factor against incident solar radiation for the smooth tube and finned tube with sharp and round edge. It is seen that the friction factor is inversely proportional to incident solar radiation. The friction factor values from 0.082 to 0.1255 for the round edge and from 0.1025 to 0.1568 the sharp edge achieved when incident solar radiation changed from  $800\text{ W/m}^2$  to  $1100\text{ W/m}^2$ . Variation of the thermal enhancement index (TEI) incident solar radiation for the sharp and round edge is shown in Fig. 12D, which indicates that the best thermal enhancement index is achieved with the round edge. At  $1100\text{ W/m}^2$ , TEI of 1.667 and 1.464 is achieved for the round edge and sharp edge; respectively. Finally, the reported results confirm that the round edge fine enhance the thermal performance of PTC.

**Table 6 Performance characteristics of finned tube as a function of solar intensity**

Solar radiation [ $\text{W/m}^2$ ]	Useful heat [kW]		Thermal efficiency [-]		Thermal loss [kW]		Pressure loss [kPa]	
	round	sharp	round	sharp	round	sharp	round	sharp
$I_b$								
800	21.425	21.333	0.6867	0.6837	2.130	2.223	3.000	3.308
850	22.851	22.753	0.6893	0.6864	2.177	2.275	2.600	2.867
900	24.243	24.139	0.6907	0.6877	2.257	2.361	2.400	2.647
950	25.635	25.525	0.6919	0.6889	2.337	2.447	2.200	2.426
1000	27.066	26.949	0.6940	0.6910	2.379	2.496	1.995	2.200
1050	28.385	28.263	0.6932	0.6902	2.531	2.653	1.800	1.985
1100	29.743	29.616	0.6933	0.6903	2.646	2.773	1.700	1.875

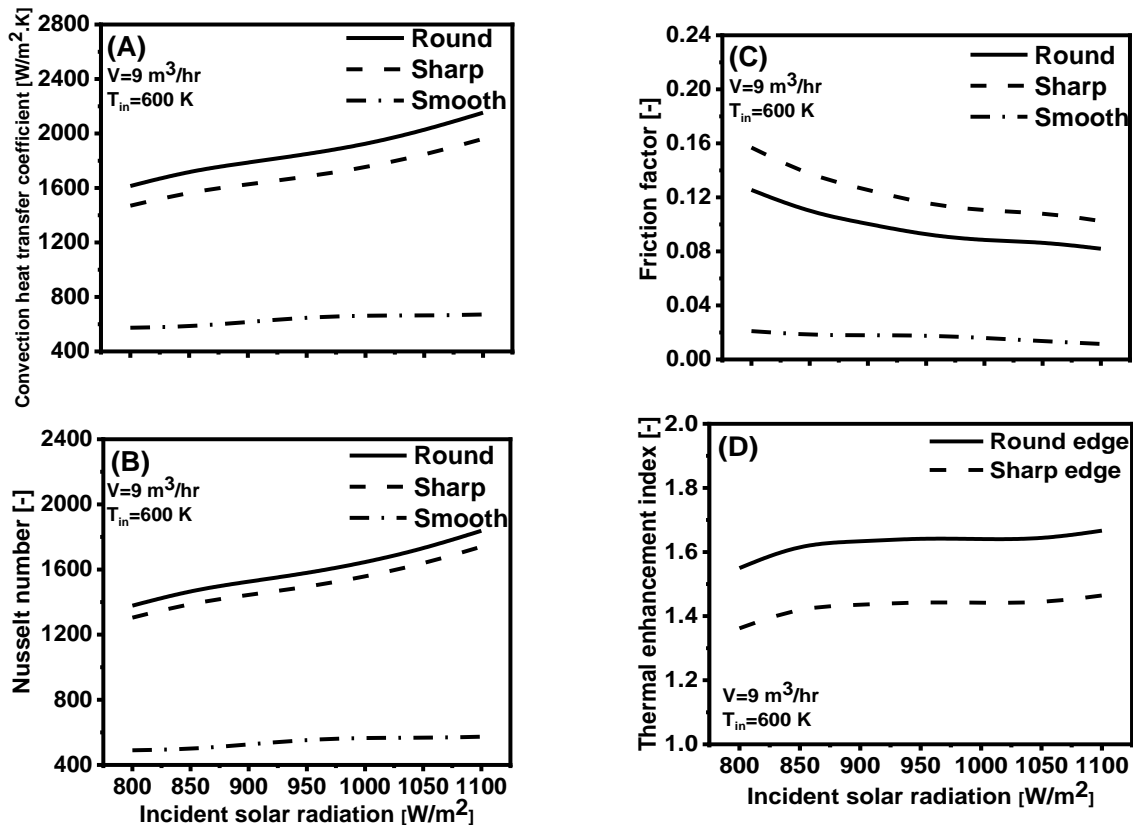


Figure 12 Variation of performance characteristics with incident solar radiation for different edge

## Conclusions

The objective of the present work is to examine the use of internal round longitudinal fins with rectangular shape inside the absorber of the LS-2 parabolic trough collector. Computational Fluid Dynamics with UDFs code is used as a simulation tool in the present work. Comparison between sharp edge and round edge is made over a wide range of operating parameters such as the inlet temperature (300:600K), the volume flow rate (9m<sup>3</sup>/h: 27m<sup>3</sup>/h) and direct normal solar irradiance (800 W/m<sup>2</sup>:1100 W/m<sup>2</sup>). Based on the reported results, the following conclusions can be drawn:

- Average of thermal enhancement index is about 1.567, 1.366 for round and sharp edge; respectively, over the considered range of inlet heat transfer fluid temperature.
- Average of thermal enhancement index is 1.376, 1.209 for round and sharp edge; respectively, over the investigated range of flow rate.
- Average of thermal enhancement index is 1.628, 1.431 for round and sharp edge; respectively, over the whole range of incident solar radiation.
- Nusselt number of the round edge (1643) is higher than that of the sharp edge (1555.72) while the friction factor of the round edge (0.088) is lower than that of the sharp edge (0.11) at the heat transfer fluid inlet temperature of 600K, flow rate of 9 m<sup>3</sup>/h and direct normal solar irradiance of 1000 W/m<sup>2</sup>.

- Convective heat transfer coefficient of the round edge (1950 W/m<sup>2</sup>K) is higher than that of the sharp edge (1775.784 W/m<sup>2</sup>K) at the heat transfer fluid inlet temperature of 600K, flow rate of 9 m<sup>3</sup>/h, and direct normal solar irradiance of 1000 W/m<sup>2</sup>.

## NOMENCLATURES

Symbol	Description	Units	Greek symbols	
A	area	m <sup>2</sup>	$\alpha$	absorber absorbance ---
C	concentration ratio	---	$\varepsilon$	emittance ---
$C_p$	specific heat at constant pressure	J/kg K	$\Delta$	difference ---
D	diameter	m	$\eta_{op}$	optical efficiency ---
F	focal length	m	$\eta_{th}$	thermal efficiency ---
f	friction factor		$\theta$	angle between fins (°) (°)
h	heat transfer coefficient	W/m <sup>2</sup> K	$\mu$	dynamic viscosity Pa s
$I_b$	solar direct beam irradiation	W/m <sup>2</sup>	$\rho$	density kg/m <sup>3</sup>
K	thermal conductivity	W/m.K	$\tau$	transmittivity ---
k	the incident angle modifier unity	---	<b>Subscripts</b>	
L	parabola length	m	a	aperature
$\dot{m}$	mass flow rate	kg/s	fm	mean fluid
Nu	Nusselt number	---	in	inlet
p	fin length	mm	loss	thermal loss
P	pressure	kPa	out	outlet
Q	heat flux	W	r	receiver
Re	Reynolds number	---	ri	inner receiver
R	rounding radius	mm	ro	outer receiver
t	fin thickness	mm	s	solar
T	temperature	°C	u	useful
V	volume flow rate	m <sup>3</sup> /h	0	smooth absorber (reference case)
W	parabola width	m		

## References

- [1] Akbarzadeh, Sanaz, and Mohammad Sadegh Valipour. "Heat transfer enhancement in parabolic trough collectors: A comprehensive review." *Renewable and Sustainable Energy Reviews* 92 (2018): 198-218.
- [2] Jaramillo, O. A., Mónica Borunda, K. M. Velazquez-Lucho, and Miguel Robles. "Parabolic trough solar collector for low enthalpy processes: An analysis of the efficiency enhancement by using twisted tape inserts." *Renewable Energy* 93 (2016): 125-141.
- [3] Mwesigye, Aggrey, Tunde Bello-Ochende, and Josua P. Meyer. "Heat transfer and entropy generation in a parabolic trough receiver with wall-detached twisted tape inserts." *International Journal of Thermal Sciences* 99 (2016): 238-257.
- [4] Chang, C., C. Xu, Z. Y. Wu, X. Li, Q. Q. Zhang, and Z. F. Wang. "Heat transfer enhancement and performance of solar thermal absorber tubes with circumferentially non-uniform heat flux." *Energy Procedia* 69 (2015): 320-327.
- [5] Ghadirijafarbigloo, Sh, A. H. Zamzamian, and M. Yaghoubi. "3-D numerical simulation of heat transfer and turbulent flow in a receiver tube of solar parabolic trough concentrator with louvered twisted-tape inserts." *Energy procedia* 49 (2014): 373-380.

- [6]Garg, M. O., Himanshu Nautiyal, Sourabh Khurana, and M. K. Shukla. "Heat transfer augmentation using twisted tape inserts: A review." *Renewable and Sustainable Energy Reviews* 63 (2016): 193-225.
- [7]Diwan, Ketan, and M. S. Soni. "Heat transfer enhancement in absorber tube of parabolic trough concentrators using wire-coils inserts." *Universal Journal of Mechanical Engineering* 3, no. 3 (2015): 107-112.
- [8]Şahin, Hacı Mehmet, Eşref Baysal, Ali Rıza Dal, and Necmettin Şahin. "Investigation of heat transfer enhancement in a new type heat exchanger using solar parabolic trough systems." *International journal of hydrogen energy* 40, no. 44 (2015): 15254-15266.
- [9]Jamal-Abad, Milad Tajik, Seyfollah Saedodin, and Mohammad Aminy. "Experimental investigation on a solar parabolic trough collector for absorber tube filled with porous media." *Renewable Energy* 107 (2017): 156-163.
- [10]Rashidi, Saman, Javad Abolfazli Esfahani, and Abbas Rashidi. "A review on the applications of porous materials in solar energy systems." *Renewable and Sustainable Energy Reviews* 73 (2017): 1198-1210.
- [11]Ghasemi, Seyed Ebrahim, and Ali Akbar Ranjbar. "Numerical thermal study on effect of porous rings on performance of solar parabolic trough collector." *Applied Thermal Engineering* 118 (2017): 807-816.
- [12]Chang, Chun, Adriano Sciacovelli, Zhiyong Wu, Xin Li, Yongliang Li, Mingzhi Zhao, Jie Deng, Zhifeng Wang, and Yulong Ding. "Enhanced heat transfer in a parabolic trough solar receiver by inserting rods and using molten salt as heat transfer fluid." *Applied Energy* 220 (2018): 337-350.
- [13]Bellos, Evangelos, and Christos Tzivanidis. "Investigation of a star flow insert in a parabolic trough solar collector." *Applied Energy* 224 (2018): 86-102.
- [14]Mwesigye, Aggrey, Tunde Bello-Ochende, and Josua P. Meyer. "Multi-objective and thermodynamic optimisation of a parabolic trough receiver with perforated plate inserts." *Applied Thermal Engineering* 77 (2015): 42-56.
- [15]Bellos, Evangelos, Christos Tzivanidis, and Dimitrios Tsimpoukis. "Multi-criteria evaluation of parabolic trough collector with internally finned absorbers." *Applied Energy* 205 (2017): 540-561.
- [16]Cheng, Z. D., Y. L. He, and F. Q. Cui. "Numerical study of heat transfer enhancement by unilateral longitudinal vortex generators inside parabolic trough solar receivers." *International journal of heat and mass transfer* 55, no. 21-22 (2012): 5631-5641.
- [17]Bellos, Evangelos, Christos Tzivanidis, and Dimitrios Tsimpoukis. "Optimum number of internal fins in parabolic trough collectors." *Applied Thermal Engineering* 137 (2018): 669-677.
- [18]Muñoz, Javier, and Alberto Abánades. "Analysis of internal helically finned tubes for parabolic trough design by CFD tools." *Applied energy* 88, no. 11 (2011): 4139-4149.
- [19]Bellos, E., C. Tzivanidis, K. A. Antonopoulos, and G. Gkinis. "Thermal enhancement of solar parabolic trough collectors by using nanofluids and converging-diverging absorber tube." *Renewable Energy* 94 (2016): 213-222.
- [20]Bellos, Evangelos, Christos Tzivanidis, and Dimitrios Tsimpoukis. "Thermal enhancement of parabolic trough collector with internally finned absorbers." *Solar energy* 157 (2017): 514-531.
- [21] Laaraba, Adel, and Ghazali Mebarki. "Enhancing Thermal Performance of a Parabolic Trough Collector with Inserting Longitudinal Fins in the Down Half of the Receiver Tube." *Journal of Thermal Science* 29, no. 5 (2020): 1309-1321.
- [22] Bellos, Evangelos, and Christos Tzivanidis. "Alternative designs of parabolic trough solar collectors." *Progress in Energy and Combustion Science* 71 (2019): 81-117.
- [23]Behar, Omar, Abdallah Khellaf, and Kamal Mohammedi. "A novel parabolic trough solar collector model–Validation with experimental data and comparison to Engineering Equation Solver (EES)." *Energy Conversion and Management* 106 (2015): 268-281.
- [24]Dudley, Vernon E., Gregory J. Kolb, A. Roderick Mahoney, Thomas R. Mancini, Chauncey W. Matthews, M. I. C. H. A. E. L. Sloan, and David Kearney. Test results: SEGS LS-2 solar collector. No. SAND94-1884. Sandia National Lab.(SNL-NM), Albuquerque, NM (United States), 1994.